Direct Observation of the Release of Phenylalanine from Diphenylalanine Nanotubes

ARTICLE *in* JOURNAL OF THE AMERICAN CHEMICAL SOCIETY · JUNE 2006

Impact Factor: 12.11 · DOI: 10.1021/ja060358g · Source: PubMed

5 AUTHORS, INCLUDING:

Victoria L Sedman
University of Nottingham
9 PUBLICATIONS **302** CITATIONS
SEE PROFILE

Stephanie Allen
University of Nottingham
124 PUBLICATIONS **2,243** CITATIONS
SEE PROFILE

Ehud Gazit
Tel Aviv University
175 PUBLICATIONS **8,772** CITATIONS
SEE PROFILE

Saul J. B. Tendler
University of Nottingham
256 PUBLICATIONS **7,444** CITATIONS
SEE PROFILE

J|A|C|S
ARTICLES
Published on Web 05/09/2006

Direct Observation of the Release of Phenylalanine from Diphenylalanine Nanotubes

Victoria L. Sedman,[‡] Lihi Adler-Abramovich,[†] Stephanie Allen,[‡] Ehud Gazit,[†] and Saul J. B. Tendler*[,‡]

Contribution from the Department of Molecular Microbiology and Biotechnology, George S. Wise Faculty of Life Sciences, Tel Aviv University, Tel Aviv 69978, Israel, and Laboratory of Biophysics and Surface Analysis, School of Pharmacy, University of Nottingham, Nottingham NG7 2RD, U.K.

Received January 17, 2006; E-mail: saul.tendler@nottingham.ac.uk

Abstract: The core recognition motif of the amyloidogenic β-amyloid polypeptide is a dipeptide of phenylalanine. This dipeptide readily self-assembles to form discrete, hollow nanotubes with high persistence lengths. The simplicity of the nanotube formation, combined with ideal physical properties, make these nanotubes highly desirable for a range of applications in bionanotechnology. To fully realize the potential of such structures, it is first necessary to gain a comprehensive understanding of their chemical and physical properties. Previously, the thermal stability of these nanotubes has been investigated by electron microscopy. Here, we further our understanding of the structural stability of the nanotubes upon dry-heating using the atomic force microscope (AFM), and for the first time identify their degradation product utilizing time-of-flight secondary-ion mass spectrometry. We show that the nanotubes are stable at temperatures up to 100 °C, but on heating to higher temperatures begin to lose their structural integrity with an apparent collapse in tubular structure. With further increases in temperature up to and above 150 °C, there is a degradation of the structure of the nanotubes through the release of phenylalanine building blocks. The breakdown of structure is observed in samples that are either imaged at elevated temperatures or imaged following cooling, suggesting that once phenylalanine is lost from the nanotubes they are susceptible to mechanical deformation by the imaging AFM probe. This temperature-induced plasticity may provide novel properties for these peptide nanotubes, including possible applications as scaffolds and drug delivery devices.

Introduction

Amyloid is the generic term given to the proteinaceous fibrillar structures found in a range of degenerative human diseases, including Alzheimer's disease, Type II Diabetes Mellitus, and Creuztfeld−Jacob's disease. Despite the diverse origins of the proteins that self-assemble as pathogenic amyloid, it has a generic supramolecular structure of stacked β-sheets in which the strands are arranged perpendicular to the fibril axis and stabilized by hydrogen bonding.[1,2] The ordered stacking within these structures is thought to be driven by aromatic stacking of side chains by $\pi-\pi$ interactions.[3−11] The intermolecular forces that stabilize amyloid are intrinsic to the stabilization of the peptide backbone, suggesting that such structures may be engineered from any peptide system.[12] As the knowledge and understanding of amyloid formation and structure has developed, it has become increasingly apparent that they have significant potential for exploitation in bionanotechnology.

The ability to control and manipulate the self-assembly processes is an ongoing endeavor in the biotechnology industry, as is the quest to find the simplest biomaterial building blocks with the best functionality and properties. A growing number of studies already demonstrate the broad range of nanostructures that can be self-assembled from simple peptides ranging from nano-spheres, -composites, -vesicles, -ribbons, and -tubes;[13−19]

[†] Tel Aviv University.
[‡] University of Nottingham.

(1) Blake, C. C. F.; Serpell, L. C. *Structure* **1996**, *4*, 989−998.
(2) Sunde, M.; Serpell, L. C.; Bartlam, M.; Fraser, P. E.; Pepys, M. B.; Blake, C. C. F. *J. Mol. Biol.* **1997**, *273*, 729−739.
(3) Gazit, E. *FASEB J.* **2002**, *16*, 77−83.
(4) Naito, A.; Kamihira, M.; Inoue, R.; Saito, H. *Magn. Reson. Chem.* **2004**, *42*, 247−257.
(5) Makin, O. S.; Atkins, E.; Sikorski, P.; Johansson, J.; Serpell, L. C. *Proc. Natl. Acad. Sci. U.S.A.* **2005**, *102*, 315−320.
(6) Tartaglia, G. G.; Cavalli, A.; Pellarin, R.; Caflisch, A. *Protein Sci.* **2004**, *13*, 1939−1941.
(7) Zanuy, D.; Nussinov, R. *J. Mol. Biol.* **2003**, *329*, 565−584.
(8) Zanuy, D.; Porat, Y.; Gazit, E.; Nussinov, R. *Structure* **2004**, *12*, 439−455.
(9) Haspel, N.; Zanuy, D.; Ma, B.; Wolfson, H.; Nussinov, R. *J. Mol. Biol.* **2005**, *345*, 1213−1239.
(10) Wu, C.; Lei, H.; Duan, Y. *Biophys. J.* **2005**, *88*, 2897−2906.
(11) Colombo, G.; Daidone, I.; Gazit, E.; Amadei, A.; Di Nola, A. *Proteins* **2005**, *59*, 519−527.
(12) Macphee, C. E.; Dobson, C. M. *J. Am. Chem. Soc.* **2000**, *122*, 12707−13.
(13) Bull, S. R.; Guler, M. O.; Bras, R. E.; Meade, T. J.; Stupp, S. I. *Nano Lett.* **2005**, *5*, 1−4.
(14) Song, Y.; Challa, S. R.; Medforth, C. J.; Qiu, Y.; Watt, R. K.; Pena, D.; Miller J. E.; van Swol, F.; Shelnutt, J. A. *Chem. Commun.* **2004**, *9*, 1044−45.
(15) Reches, M.; Gazit, E. *Nano Lett.* **2004**, *4*, 581−85.
(16) Tjernberg, L.; Hosia, W.; Bark, N.; Thyberg, J.; Johansson, J. *J. Biol. Chem.* **2002**, *277*, 43243−6.
(17) Zhang, S. *Nat. Biotechnol.* **2003**, *21*, 1171−8.
(18) Zhang, S.; Marini, D. M.; Hwang, W.; Santoso, S. *Curr. Opin. Chem. Biol.* **2002**, *6*, 865−71.
(19) Vauthey, S.; Santoso, S.; Gong, H.; Watson, N.; Zhang, S. *Proc. Natl. Acad. Sci. U.S.A.* **2002**, *99*, 5355−60.

10.1021/ja060358g CCC: $33.50

these have been explored for their potential utilization as matrixes for chromatography or screening, contrast agents for magnetic resonance, scaffolds for tissue engineering, and nanowires in microelectronics.

To fully realize the potential of such structures, it is important to understand the integral chemical and physical properties of these nanostructures. Here, we focus on the investigations of the properties of the nanotubes formed by a simple aromatic dipeptide. Investigations by Reches and Gazit[20] led to the discovery that the core recognition motif of β-amyloid protein, a simple dipeptide of L-phenylalanine $NH_2-Phe-Phe-COOH$ (FF), readily self-assembles into tubular nanostructures. A dipeptide of D-phenylalanine also formed nanotubular assemblies of identical structural properties.[20]

The FF nanotubes are efficiently formed under mild conditions, thus offering the potential for low-cost bulk manufacturing. A model for FF nanotube assembly suggests that the nanotubes are similar to fullerene and carbon nanotubes in their formation from a flat two-dimensional sheet stabilized by the interactions of aromatic ring side chains, which direct order during assembly by $\pi-\pi$ stacking. The formation of the extended β-sheet is further stabilized by the aromatic interactions and hydrogen bonding. The tubular structure is formed by the closure and stabilization of the β-sheet by further interactions.[15] Electron microscopy and atomic force microscopy (AFM) studies have shown that the nanotubes are hollow water-filled structures[20,21] ranging in dimensions from 50 to 1000 nm in diameter and are discrete nanotubes with no branching. Investigations into the physical properties of the nanotubes will provide further information as to their potential for a variety of applications, including taking advantage of their high persistence lengths and strength relative to other bionanomaterials; they have a Young's modulus of about 20 GPa.[21] Studies also suggest[14] that the FF nanotube walls are porous, thus opening up a new avenue of applications as functionalized composite material or drug delivery devices.

The thermal and chemical stability of the FF nanotubes has recently been studied, in ambient and dry heat conditions, using a range of analytical techniques.[22] Importantly, FF nanotubes were shown to be stable to heating in an autoclave. However, high-resolution electron microscopy revealed the degradation of the nanotubes at temperatures in excess of 150 °C. To understand this phenomenon at a structural and chemical level, we have now further investigated the stability of such FF nanotubes. The thermal stability was studied by in situ and ex situ heating of the sample using the AFM. Further analysis of the resultant artifacts of heating was investigated by time-of-flight secondary-ion mass spectrometry (TOF-SIMS).

Experimental Section

Preparation of Peptide Samples. FF peptides were purchased from Bachem (Bubendorf, Switzerland). Fresh stock solutions were prepared by dissolving the lyophilized peptides in 1,1,1,3,3,3-hexafluoro-2-propanol (Sigma Aldrich) at a concentration of 100 mg/mL. Peptide stock solution was diluted in double distilled (dd) H_2O to a final concentration of 2 mg/mL. To prevent overcrowding of the scan area, samples were diluted in Elgar water to a final concentration of 0.2 or 1 mg/mL prior to dropping a 10 μL aliquot onto freshly cleaved mica and were subsequently dried in a vacuum generator.

Atomic Force Microscopy. AFM images were generated using a Nanoscope IIIa AFM (Digital Instruments, Veeco Metrology Group, Santa Barbara, CA). All imaging was performed in air using the J-type scanner with heating stage using silicon TESP cantilevers (supplied by Veeco Metrology Group) mounted on cantilevers with nominal spring constants of 42 N/m and resonant frequency of 320 kHz. Scan rates employed were 0.5−0.8 Hz, and scan sizes were 10 μm × 10 μm. Data were analyzed using the SPIP program (Image Metrology ApS).

In Situ Heat Imaging. The sample stage has an internal heater, which from the bottom up heats the sample and the enclosed space within the specialized AFM cell. The temperature of the system is monitored by the built-in thermometer and maintained by the feedback coolant system. Samples were heated in situ using a heating stage incorporated into the J-scanner of the AFM. Samples were placed onto the stage and initially imaged at room temperature. The temperature was then increased to 25, 50, 100, 150, and 200 °C. Following each temperature increase, the system was allowed to equilibrate for 5 min and then the temperature was maintained throughout imaging. Immediately after each image was captured, the temperature was increased.

Ex Situ Heat Imaging. The same AFM experimental setup was used as for imaging in situ with the exception that samples were heated to the desired temperature, allowed to equilibrate for 5 min, and then cooled and equilibrated for a further 5 min prior to imaging at 25 °C.

TOF-SIMS Analysis. TOF-SIMS (time-of-flight secondary-ion mass spectrometer, ION-TOF GmbH, Germany) was used to analyze crystalline material that was observed to form on the cantilever at high temperatures. The primary ion source used was a Ga beam with kinetic energy of 15 kV (20 μA), which delivers Ga+ cluster ions over a raster scan area of 300 × 300 μm^2. High-resolution mass spectra and secondary ion images were generated of the cantilever and chip surface.

Optical images of the cantilevers were generated using the Leica TCS Confocal microscope (Leica Microsystems (U.K.) Ltd.) at ×2.5 and ×10 magnification.

Results

In Situ Heat Imaging. The thermal stability of the nanotubes was investigated in situ by increasing the temperature of the sample by regular increments to the desired temperature, and after an equilibrium period an AFM image was recorded before the temperature was again raised. Several different nanotube samples were examined. Figure 1a−d shows the variation in morphology of the same exemplar nanotube as the temperature was increased with the imaging parameters kept as constant as possible. The graphs displayed in Figure 1e and f show the average dimensions of the nanotube cross-sections; Figure 1e shows the change in nanotube half-height widths with temperature, and Figure 1f shows the change in peak height of the nanotube with temperature. Cross-sectional analysis of the nanotube shows that the morphology and dimensions remain constant at temperatures below 100 °C (Figure 1a,b). However, at 100 °C, wall integrity starts to break down and the nanotube appears to deform with a visible trough in the top of the cross-section profiles (Figure 1c). Also, considerable variation in morphology along the nanotube axis occurs with loss of its smooth outer wall topography. On increasing the temperature further to 150 °C, the nanotube loses spatial volume, resulting in structures resembling flattened nonuniform ribbons with an 82% loss in nanotube height and a 66% decrease in width. Regions of high and low topography were observed; however, a constant width was observed along the nanotube (Figure 1d).

(20) Reches, M.; Gazit, E. *Science* **2003**, *300*, 625−7.
(21) Kol, N.; Adler-Abramovich, L.; Barlam, D.; Shneck, R. Z.; Gazit, R.; Rousso, I. *Nano Lett.* **2005**, *5*, 1343−1346.
(22) Adler-Abramovich, L.; Reches, M.; Sedman, V. L.; Allen, S.; Tendler, S. J. B.; Gazit, E. *Langmuir* **2006**, *22*, 1313−20.

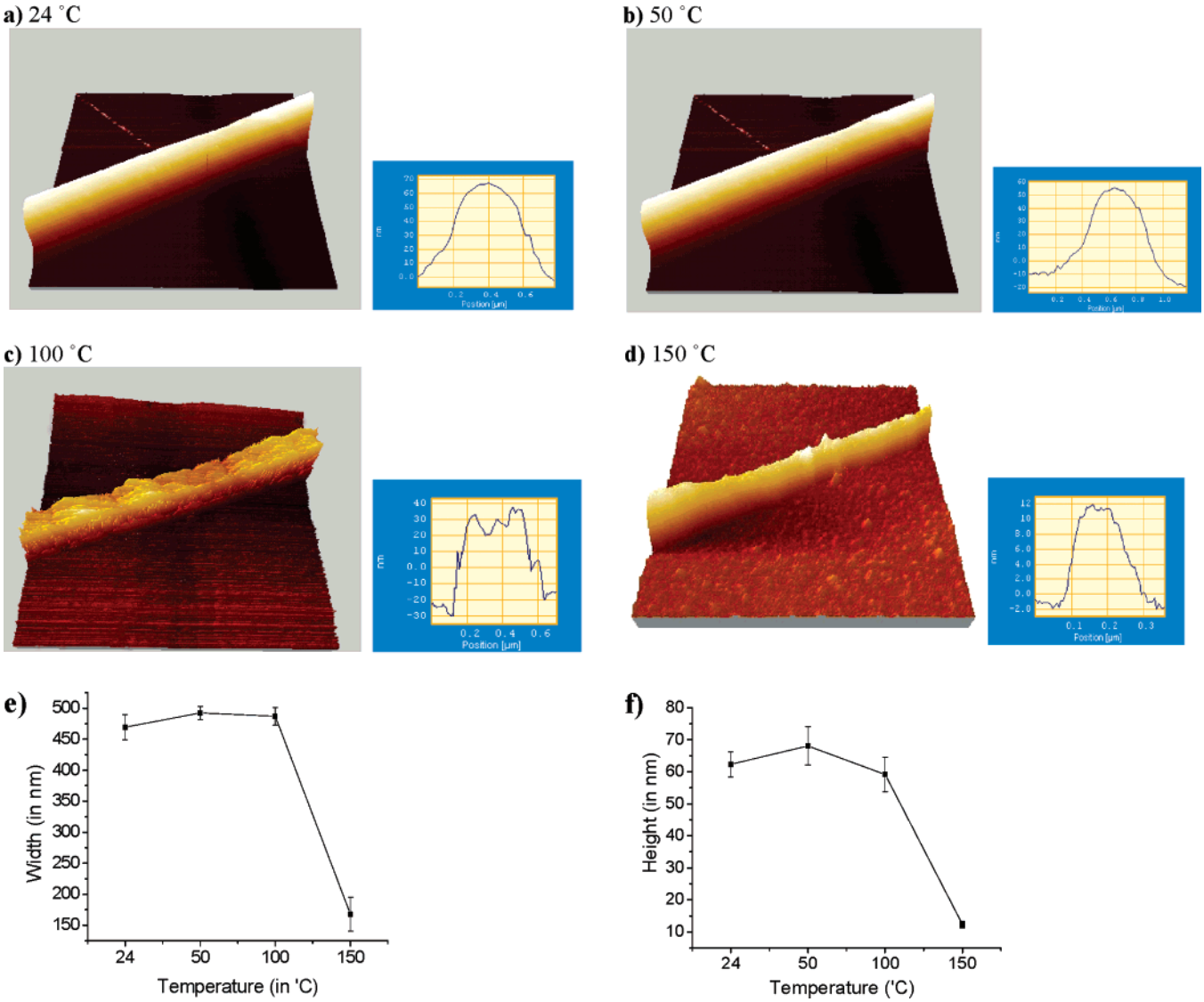

Figure 1. High-temperature AFM images of peptide nanotubes. 3D topography images (5 μm × 5 μm) of a peptide nanotube when heated to 24 (a), 50 (b), 100 (c), and 150 °C (d). Samples were heated to relative temperature, allowed to equilibrate for 5 min, and then imaged at constant temperature. Insets show the cross-sectional profile of the nanotube and the topography profile along the axis of the nanotube. (e) The change in widths at nanotube half-height with temperature; (f) the change in nanotube height with temperature.

In addition, the 150 °C image shows that granular material has been deposited onto the substrate and that regions of the nanotube appear to have amorphous material deposited along its length. For temperatures above 150 °C, it was not possible to produce stable AFM images. On further investigation of the AFM cantilevers using confocal microscopy, it was found that during the heating and/or imaging process a crystalline material had deposited onto the cantilevers (Figure 3). Investigation into the origins and composition of the material was undertaken using TOF-SIMS.

Ex Situ Heat Imaging. To investigate whether the observed loss of nanotube integrity while imaging at high temperatures was a result of the mechanical forces imposed by the AFM probe during imaging, samples were heated and then allowed to cool prior to imaging at room temperature. Figure 2a−d shows AFM images of peptide nanotubes self-assembled at room temperature, deposited onto freshly cleaved mica and heat-treated. The graphs in Figure 2e and f show the average dimensions of the nanotube cross-sections; Figure 2e shows the change in nanotube half-height widths with temperature, and Figure 2f shows the change in peak height of the nanotube with temperature. The AFM images show that the nanotubes morphology remains similar at temperatures up to 100 °C with no noticeable loss in the nanotubes dimensions (Figure 2a, b, e, and f). However, as the temperature was increased further, at 125 °C there is some change in surface topography (Figure 2c) together with a slight decrease in nanotube height (Figure 2f). A continued increase in temperature up to 150 °C caused a noticeable loss in nanotube integrity with a loss of 81% of nanotube height. The resultant morphologies were not uniform along the nanotube axis and appeared as pockets of narrow and wide segments with reduced dimensions; this contributes to the error measurement in these data points in Figure 2e. Again, the surface of the mica appears to have a granular deposit.

When samples were heated to 200 °C, again some crystalline debris was observed on the cantilever but to a lesser extent than the previous high-temperature imaging experiment. This reduced deposition could be attributed to the tip not being in contact with the sample at high temperatures and as such the cantilever being further away from the sample during heating. As with

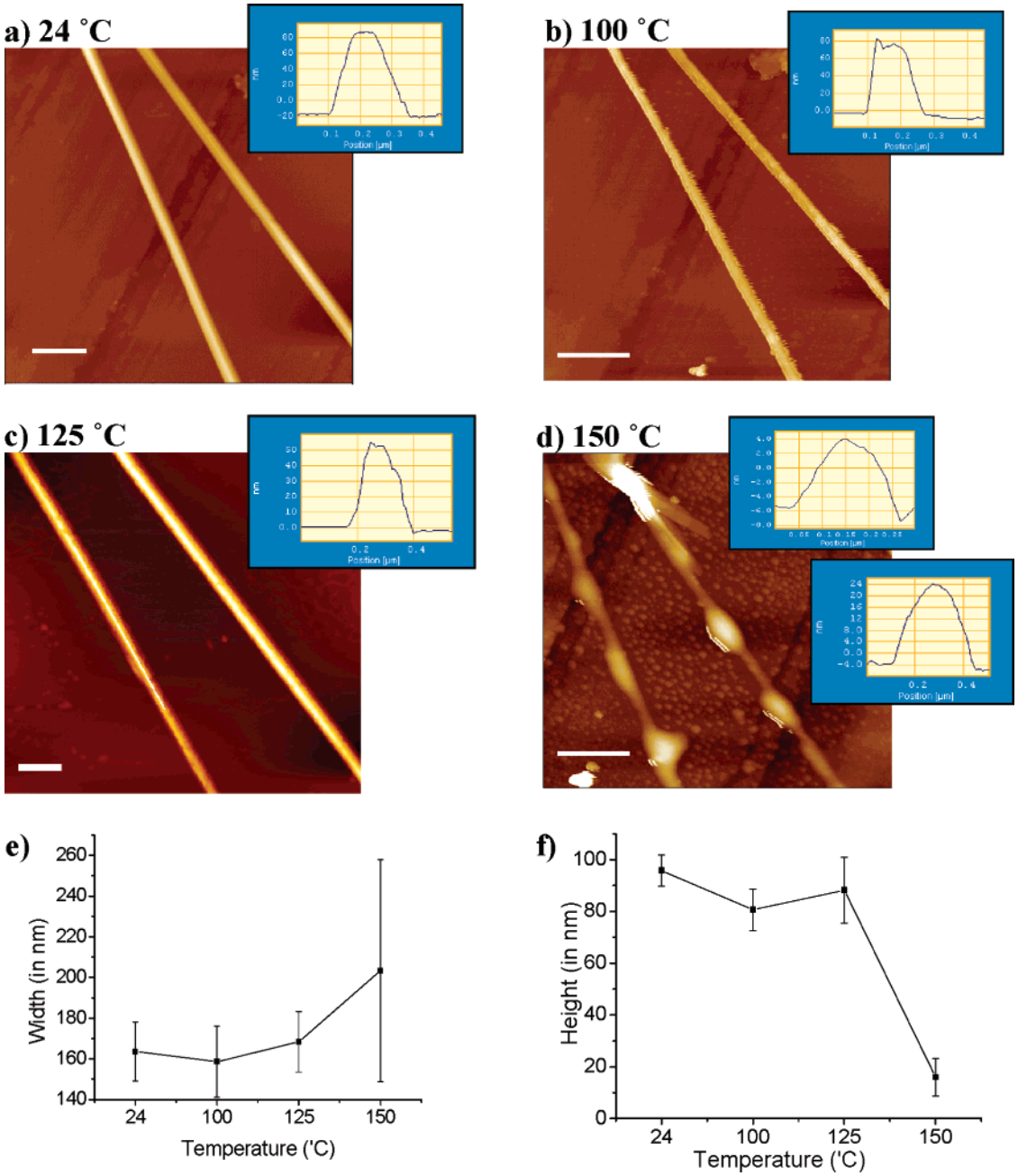

Figure 2. AFM images of heat-treated peptide nanotubes. Topography images of peptide nanotubes when heated to 24 (a), 100 (b), 125 (c), and 150 °C (d). Samples were heated successively to relative temperature, equilibrated for 5 min, and then allowed to cool for 5 min before imaging at 25 °C. Scale bars represent 1 μm. Insets show the cross-sectional profile of left-hand nanotube. Part (c) shows two cross-sectional profiles highlighting the relative difference between the narrow and thicker pockets of the nanotube. (e) The change in widths at nanotube half-height with temperature; (f) the change in nanotube height with temperature.

the in situ imaging experiment, it is suggested that this deposition prevented the generation of stable AFM images.

TOF-SIMS. The crystalline material deposition was widespread on both the cantilever and the chip, with particular concentration of large protruding deposits around the "tip" region of the cantilever (Figure 3). During imaging, these structures are likely to act as multiple faux tips on the cantilever as well as interfere with the laser beam reflection from the cantilever, all of which contributed to the loss of stable imaging of the sample.

The positive spectrum for the TOF-SIMS analysis of the cantilevers is shown in Figure 4a. Despite extensive cleaning of the silicon cantilevers by a process of plasma etching (20 Pa O_2, 100 W for 60 s) and UV cleaning prior to imaging, a residual contamination of poly(dimethylsiloxane) (PDMS) was found to be present on the cantilevers, most likely originating from their packaging conditions. However, on subtraction of the peaks corresponding to the contamination (spectrum reference for PDMS from The Static SIMS Library (SurfaceSpectra Ltd.) for PDMS oil and rubber), three peaks of interest may be observed in the positive sample spectra at *m*/*u* of 77, 91, and 120. These molecular weights correspond to hydrocarbon compounds of C_6H_5, C_7H_7, and $C_8H_{10}N$, respectively; these structures can be commonly attributed to varying degrees of fragmentation of phenylalanine, specifically fragments of, or containing, the aromatic ring side-chain (Figure 4b).

Figure 3. Optical image of the crystalline deposits on AFM cantilever after heat treatment of peptide nanotubes. Optical image was generated using a Leica TCS confocal microscope with ×2.5 and ×10 lens.

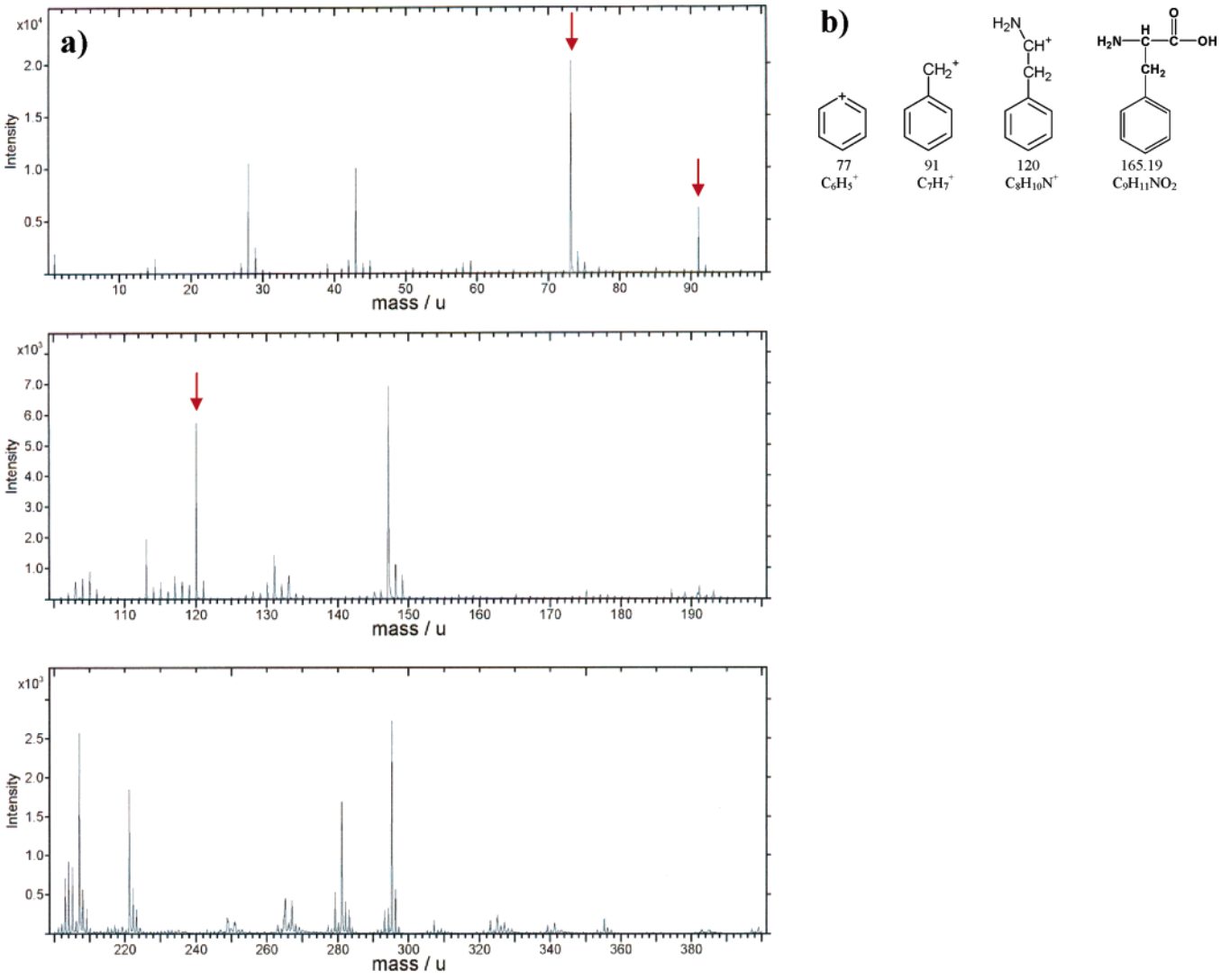

Figure 4. TOF SIMS spectra of the crystalline deposits on the AFM cantilevers following heat treatment of the peptide nanotubes. Part (a) is the positive TOF SIMS spectrum of the crystalline debris on the AFM cantilevers, with peaks of interest highlighted at *m*/*u* of 77, 91, and 120. (b) Suggested chemical structures of the molecules corresponding to these peaks and the structure of phenylalanine (far right).

Discussion

The core recognition motif of the β-amyloid protein, a dipeptide of FF, efficiently self-assembles into discrete hollow nanotubes. These nanotubes have previously been investigated for their application in microelectronics as degradable scaffolds for the production of nanowires.[20] Under standard conditions, the FF nanotubes display a high degree of rigidity and strength with an averaged point stiffness of 160 N/m and Young's modulus of 19 GPa as measured by AFM.[21] Under standard conditions, the nanotubes can be repeatedly imaged by AFM and display no noticeable deterioration in the morphology or dimensions of the nanotubes.[20−22]

In a previous study,[22] the thermal and chemical stability of FF nanotubes was investigated. The data we present here complement the findings of the study in which the thermal stability of the FF nanotubes was investigated under wet conditions (following autoclaving at 121 °C, 1.2 atm). The EM and AFM data of the samples after autoclaving show that the FF nanotubes remained structurally intact. However, high-resolution electron microscopy revealed the degradation of the nanotubes at temperatures in excess of 150 °C. This study confirms by AFM that when the FF nanotubes are subjected to a dry heat at similar temperatures, they appear to lose structural integrity particularly during prolonged heating at 150 °C.

The presented data clearly show that structural changes occur as the FF nanotubes are heated above 100 °C. In particular, this study focuses on a number of FF nanotubes that have been studied throughout at elevated temperatures. The dimensions of individual FF nanotubes vary considerably within any sample, with no two nanotubes having the same height or width. Because of the nature of the experiment, it is not possible to reheat the same nanotube. The nanotubes presented in Figures 1 and 2 are from different samples but were chosen on the basis of their similarity in dimensions to allow a more quantitative representation and comparison of the effects of different types of heating observed on all of the nanotubes within the samples. The results clearly indicate the collapse of the nanotubes as they are progressively heated. At the same time, it is clear that in the image recorded in Figure 1d significant granular material has been deposited upon the mica substrate and that the cylindrical nature of the nanotubes has become degraded with the tubes becoming decorated.

It is possible that this deformation is a result of the elevated temperature making the nanotubes more deformable and that they became distorted by the AFM probe as part of the imaging process. Comparison of the in situ and ex situ data strongly suggests that at higher temperatures the nanotubes degrade and that the deformation is not due solely to the mechanical force of the oscillating AFM tapping tip. The AFM tapping tips used have a nominal spring constant of 42 N/m and were raster scanned across the sample surface at a rate of 0.5−0.8 Hz with an oscillating downward tapping frequency of 320 kHz. In both the in situ (Figure 1f) and the ex situ heating data (Figure 2f), the nanotubes undergo the same dramatic loss of ∼80% in their heights. This result suggests that heat and not AFM probe contact is the controlling factor; however, once heated to 150 °C the tube may be deformed by the AFM probe no matter what temperature the sample is imaged at.

The unexpected and novel appearance of crystalline deposits on the cantilever and granular material on the substrate and nanotubes following exposure to high temperatures is consistent with the loss of nanotube integrity through chemical degradation. A previous study[22] using thermo-gravimetric analysis (TGA) noted an initial loss in mass of an FF nanotube sample at around 50 °C followed by a steady loss in nanotube mass as the temperature was increased further due to water loss from the hollow tubes. Together these findings and our AFM images suggest that at temperatures up to 100 °C, changes in nanotube integrity are due to loss of water from the FF nanotubes. By increasing the temperature up to 150 °C, a further loss in nanotube integrity was observed in both the in situ and the ex situ heating experiments. These images can be interpreted in the context of the TGA data[22] for higher temperatures, in which at approximately 150 °C an acute loss of 10% in nanotube mass is observed followed by a plateau at 175 °C until a dramatic loss in mass above 300 °C. Together with our TOF-SIMS analysis of the cantilevers, the evidence importantly suggests that at temperatures at and above 150 °C, the loss in mass and the apparent degradation in nanotube morphology is due to the loss of free phenylalanine. We suggest that it is the heat-induced loss of phenylalanine that causes the loss of structural integrity of the FF nanotubes. The growth of the crystals on the AFM cantilevers requires phenylalanine molecules and their fragments to sublime from the sample to the cantilever within the AFM instrument. The literature indicates that phenylalanine sublimes at a temperature of 130 °C under vacuum, and decomposes at 283 °C. By comparison, diphenylalanine does not sublime.[23]

The data therefore suggest that thermal degradation of FF building blocks results in the loss of free phenylalanine from the nanotubes and gives rise to a loss in nanotube structural integrity. AFM micrographs indicate that as the temperature is increased the nanotubes appear to deform, suggesting that the walls are collapsing and then as the temperature is further increased there is sublimation of the phenylalanine building block resulting in an observed flattened ribbon-like structure.

These results suggest that it may be possible to use heat and local mechanical probes to actively deform FF nanotubes. In addition, the loss of phenylalanine from the tubes suggests that they might have some future application as biodegradable drug delivery devices or scaffolds for tissue engineering applications.

Acknowledgment. V.L.S. thanks the U.K. Biotechnology and Biological Sciences Research Council for supporting her doctoral studies. Frank Rutten is thanked for recording TOF-SIMS spectra. E.G. thanks the Israel Science Foundation (F.I.R.S.T. program) for financial support.

JA060358G

(23) *The Merck Index*, 11th ed.; Centennial Edition; Budavari, S., Ed.; Merck & Co. Inc.: Rahway, NJ, 1989.